Probing Secret Interactions of Astrophysical Neutrinos in the High-Statistics Era

Ivan Esteban [ID],[1, 2, *] Sujata Pandey [ID],[3, †] Vedran Brdar [ID],[4, 5, ‡] and John F. Beacom [ID][1, 2, 6, §]

[1]*Center for Cosmology and AstroParticle Physics (CCAPP),*
Ohio State University, Columbus, Ohio 43210, USA
[2]*Department of Physics, Ohio State University, Columbus, Ohio 43210, USA*
[3]*Discipline of Physics, Indian Institute of Technology,*
Indore, Khandwa Road, Simrol, Indore - 453 552, India
[4]*Fermi National Accelerator Laboratory, Batavia, IL, 60510, USA*
[5]*Northwestern University, Department of Physics & Astronomy,*
2145 Sheridan Road, Evanston, IL 60208, USA
[6]*Department of Astronomy, Ohio State University, Columbus, Ohio 43210, USA*

Do neutrinos have sizable self-interactions? They might. Laboratory constraints are weak, so strong effects are possible in astrophysical environments and the early universe. Observations with neutrino telescopes can provide an independent probe of neutrino self ("secret") interactions, as the sources are distant and the cosmic neutrino background intervenes. We define a roadmap for making decisive progress on testing secret neutrino interactions governed by a light mediator. This progress will be enabled by IceCube-Gen2 observations of high-energy astrophysical neutrinos. Critical to this is our comprehensive treatment of the theory, taking into account previously neglected or overly approximated effects, as well as including realistic detection physics. We show that IceCube-Gen2 can realize the full potential of neutrino astronomy for testing neutrino self-interactions, being sensitive to cosmologically relevant interaction models. To facilitate forthcoming studies, we release `nuSIProp`, a code that can also be used to study neutrino self-interactions from a variety of sources. [Q]

I. INTRODUCTION

Neutrinos, ubiquitous but elusive, remain mysterious. Though many of their properties are known, we still do not know if they might have large self-interactions, also known as neutrino secret interactions (νSI) [1–4]. In that scenario, neutrinos interact with a light boson, increasing the neutrino-neutrino scattering rate with respect to that of the standard model. Laboratory limits, mostly from meson-decay experiments, are relatively weak [5, 6], allowing νSI to have large effects, potentially explaining short baseline neutrino anomalies [7–12] and the muon $g - 2$ anomaly [13–17].

Allowed νSI would dramatically affect the evolution of systems with high neutrino densities, such as supernovae [18] and the early universe [4, 19–22]. While cosmological measurements have robustly established the presence of a radiation background compatible with expectations for the cosmic neutrino background (CνB) [23, 24], its dynamics are poorly constrained. In fact, Ref. [25] found a *preference* for νSI in the Planck cosmic microwave background (CMB) data that could help alleviate the H_0 and σ_8 tensions [23, 26] (but see Refs. [27–31], where it is argued that polarization data restrict this possibility). Regardless of the outcome of that debate, it illustrates that a full understanding of possible νSI is critical to our understanding of the early universe, especially in the upcoming high-precision cosmology era [32–36].

Figure 1 shows another essential point about νSI: while the constraints are strong for ν_e, they are incomplete for ν_μ and nearly nonexistent for ν_τ (this figure is explained in detail in Sec. II). This is why large cosmological effects from νSI remain allowed.

A new opportunity to probe νSI has arisen due to the detection of high-energy neutrinos by IceCube [37–39]. The basic idea is that scattering of astrophysical neutrinos with the CνB en route to Earth redistributes their energies, leading to dips and bumps in the detected spectrum of the diffuse astrophysical neutrino background. Because we now know that all mass eigenstates have substantial ν_τ components [40–42], this provides a new tool to explore ν_τ self-interactions beyond the reach of laboratory experiments. However, with the relatively low statistics of IceCube data [43, 44], it is hard to realize the full potential of this technique.

In this paper, we define a roadmap for making decisive progress. The first key to this is the proposed IceCube-Gen2 (Gen2 for brevity) detector [45]. As shown below, its principal advantage relative to IceCube, beyond its better statistics, is its much wider energy range. The second key is an improved theoretical treatment. We define the observable signatures of allowed flavor-dependent νSI, correcting errors and omissions in prior work. All calculations are done without any approximation, following careful optimizations. The third key is a realistic treatment of the detector response, using code provided by IceCube. To make future studies easier, we make our code publicly available at this URL [Q].

This paper is organized as follows. In Section II, we present the theoretical description of νSI, the relevance of different effects, and the interplay with other experimen-

*Electronic address: esteban.6@osu.edu
†Electronic address: phd1501151007@iiti.ac.in
‡Electronic address: vedran.brdar@northwestern.edu
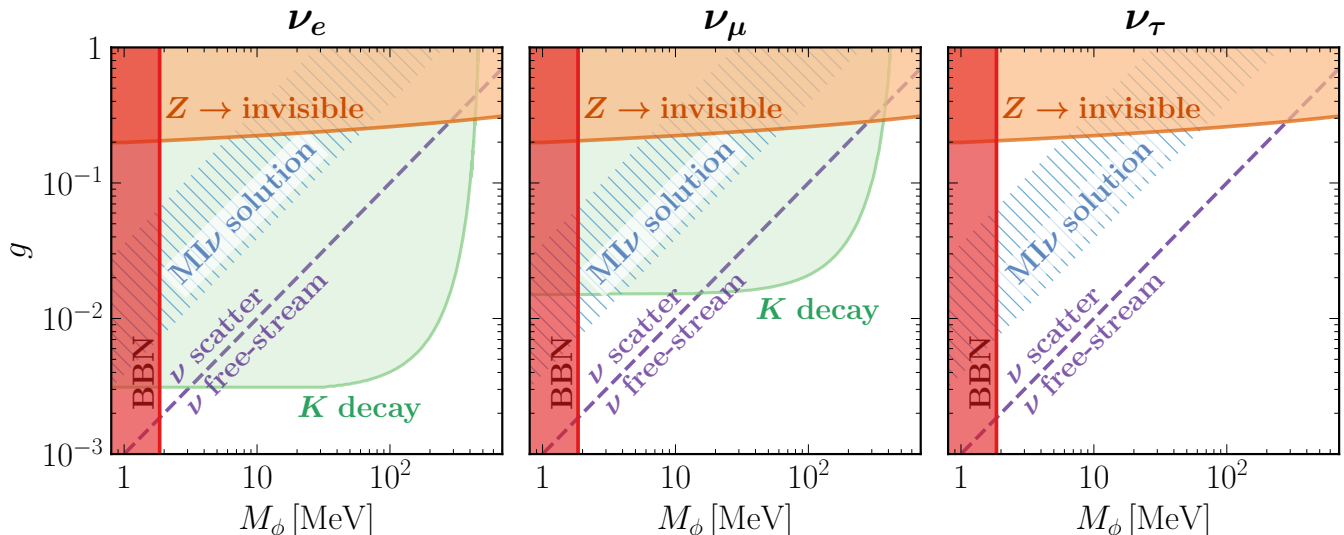§Electronic address: beacom.7@osu.edu

FIG. 1: Present constraints on neutrino self-interactions, with coupling strength g and mediator mass M_ϕ, for each of the three neutrino flavors (i.e., separately for $g_{e\alpha}$ [left], $g_{\mu\alpha}$ [center] and $g_{\tau\alpha}$ [right], for $\alpha \in \{e, \mu, \tau\}$). The hatched region is the "Moderately Interacting neutrino" (MIν) solution [6, 25], argued to affect CMB observables. The dashed purple line is the interaction strength below which cosmic neutrinos free-stream as expected at cosmologically relevant times (see text for details). Above this line, our understanding of the early universe would be affected. *As shown, ν_τ self-interactions are the least explored, leaving room for significant cosmological neutrino effects.*

tal observations. In Section III, we simulate the prospects of Gen2 to probe νSI. We show that Gen2 can probe the ν_τ and other flavor sectors with sensitivity comparable to that of laboratory studies of the ν_e sector. Thus, a combination of observables can fully probe the range of νSI that would significantly affect the dynamics of the cosmic neutrino background. In Section IV, we conclude and highlight future directions. In Appendix A, we give the results of the full νSI cross-section calculation.

II.   SECRET NEUTRINO INTERACTIONS

In this section, we define the specific νSI models we consider. Section II A introduces the theoretical description and flavor-dependent bounds on νSI. Section II B specifies the spectral signatures that we expect given our present understanding of neutrino masses and mixings. Finally, in Section II C, we demonstrate, by computing the full νSI cross-section, the relevance of previously ignored effects both in the theoretical and observed high-energy astrophysical neutrino spectrum.

A. νSI Model and Conceptual Framework

We consider νSI parametrized by the Lagrangian

$$\mathcal{L} \supset -\left(\frac{1}{2}\right) \sum_{\alpha,\beta} g_{\alpha\beta} \bar{\nu}_\alpha \nu_\beta \phi + \frac{1}{2}\partial_\mu \phi\, \partial^\mu \phi - \frac{1}{2}M_\phi^2 \phi^2 , \quad (1)$$

where ν_α are neutrino flavor eigenstates ($\alpha \in \{e, \mu, \tau\}$), $g_{\alpha\beta}$ is the interaction strength between flavors α and β, ϕ is the interaction mediator (that for simplicity we assume to be real), M_ϕ is its mass, and the $(1/2)$ prefactor is present if neutrinos are Majorana fermions. We write the coupling strength in the flavor basis, as in this basis laboratory constraints are simpler to express. This is related to the coupling in the mass basis by $g_{ij} = \sum_{\alpha,\beta} g_{\alpha\beta} U^*_{\alpha i} U_{\beta j}$, where U is the leptonic mixing matrix and $i \in \{1, 2, 3\}$.

We assume scalar interactions, as pseudoscalar interactions give the same results at high energies and vector interactions are strongly constrained from laboratory experiments [46, 47] and Big Bang Nucleosynthesis [6]. Although the Lagrangian in Eq. (1) is not gauge invariant due to the new couplings affecting neutrinos but not charged leptons, in this paper we are only interested in the low-energy phenomenology effectively described by Eq. (1). For possible UV completions that do not generate large couplings to charged leptons, see Refs. [6, 48–50]. These UV completions might induce additional signatures such as relatively large mixings with sterile neutrinos or a modified Higgs phenomenology, but these are beyond the scope of this work. We assume Majorana neutrinos, as for Dirac neutrinos stronger BBN constraints would apply [6] (see Section II B for comments on the phenomenology of Dirac neutrinos).

Figure 1 shows that νSI, particularly in the ν_τ sector, are poorly constrained and can affect our understanding of the early universe. The present constraints (at 2σ) are shown in shaded contours, which come from Z-boson decay [51], $K \to \mu\nu$ and $K \to e\nu$ decays [6, 48, 52],

and Big Bang Nucleosynthesis (BBN; obtained with the `AlterBBN 2.2` code [53, 54]). To show the scale where early-universe effects become important, the dashed purple line indicates the interaction strength below which cosmological neutrinos free-stream as expected when the largest CMB multipoles observed by Planck ($\ell \sim 2500$) enter the horizon. [1] As an example of νSI that is presently allowed, the hatched region indicates the Moderately Interacting Neutrino (MIν) solution, which has been argued to affect cosmological parameter extraction from CMB data [6, 25], especially the Hubble constant H_0 and the amplitude parameter σ_8. Even if the MIν solution fades away once more data is accumulated (there seem to be indications in that direction from Planck polarization data [27–31]), it will remain important to probe the full parameter space above the purple dashed line.

The weakest νSI constraints are in the ν_τ sector. Because of flavor mixing, astrophysical neutrinos must always contain a large ν_τ component. In what follows, we explore how νSI affect astrophysical neutrino propagation, assuming that νSI apply only in the ν_τ sector, i.e., $g_{\alpha\beta} = g\, \delta_{\alpha\tau}\delta_{\beta\tau}$ (our code `nuSIProp`, though, can handle new couplings in all sectors). In Section III, we comment how our results in fact provide comparable sensitivity to all three neutrino flavors.

The basic physics of νSI affecting astrophysical neutrino propagation is as follows. En route to Earth, high-energy astrophysical neutrinos may scatter with neutrinos in the CνB. (In the standard model, scattering is irrelevant except perhaps at ultra-high energies through the Z resonance [55, 56].). As a consequence, high-energy neutrinos are absorbed and lower-energy neutrinos are regenerated. This leads to unique dips and bumps in the astrophysical neutrino spectrum.

To quantify this description, we must follow the comoving differential neutrino number density per unit energy E_ν, dn/dE_ν, as it evolves as a function of cosmological time t. Since neutrino oscillation lengths are much smaller than astrophysical scales, flavor oscillations are quickly averaged out. We can thus follow the comoving differential density of neutrinos of mass eigenstate $i \in \{1, 2, 3\}$, $dn_i/dE_\nu \equiv \tilde{n}_i(t, E_\nu)$. This evolution is dictated by a transport equation [38, 57–59]

$$\frac{\partial \tilde{n}_i(t, E_\nu)}{\partial t} = \frac{\partial}{\partial E_\nu} \left[H(t)\, E_\nu\, \tilde{n}_i(t, E_\nu) \right] + \mathcal{L}_i(t, E_\nu)$$
$$- \tilde{n}_i(t, E_\nu) \sum_j n_j^t \sigma_{ij}(E_\nu) \qquad (2)$$
$$+ \sum_{j,\,k,\,l} n_j^t \int_{E_\nu}^{\infty} dE_\nu' \, \tilde{n}_k(t, E_\nu') \frac{d\sigma_{jk \to il}}{dE_\nu}(E_\nu', E_\nu) .$$

---

[1] To be conservative, we assume that neutrinos free-stream if $\Gamma_\nu = 0.1H$ when $(k/a)^{-1} = 10H^{-1}$, where Γ_ν is the neutrino self-interaction rate, H the Hubble parameter, k the comoving wavenumber corresponding to $\ell \sim 2500$, and a the scale factor.

The first term on the right-hand side accounts for the energy redshift due to cosmological expansion; H is the Hubble parameter. The second term represents the production rate of high-energy neutrinos from astrophysical sources: we assume it follows the star formation rate [60, 61] as a function of time, and a power law $\propto E_\nu^{-\gamma}$ with spectral index γ as a function of energy. The first two terms would thus describe the evolution of astrophysical neutrinos en route to Earth without new physics. The third term accounts for absorption due to νSI, while the fourth term accounts for the subsequent regeneration. In this equation, $n_i^t \simeq 2 \times 56\,(1+z)^3\,\mathrm{cm}^{-3} = 8.7\,(1+z)^3 \times 10^{-13}\,\mathrm{eV}^3$ is the CνB density of ν_i with z the cosmological redshift, $\sigma_{ij}(E_\nu)$ is the absorption cross-section of an incident ν_i with energy E_ν on a target ν_j, and $\sigma_{jk \to il}(E_\nu', E_\nu)$ is the cross-section for an incident ν_j with energy E_ν' on a target ν_k to generate a *detectable* ν_i with energy E_ν, along with a ν_l. For Majorana neutrinos, all final states are detectable; for Dirac neutrinos, neutrinos must be left-handed and antineutrinos right-handed.

By solving this differential equation with the initial condition $\tilde{n}_i(z \to \infty, E_\nu) = 0$, we evaluate $\tilde{n}_i(z = 0, E_\nu) \equiv \phi_i(E_\nu)$, the neutrino flux at Earth with energy E_ν. The details on how we numerically solve Eq. (2) are given at this URL ♺.

B. νSI Effects on the Spectrum

Qualitatively, the effects of νSI can be understood through the s-channel neutrino-neutrino scattering cross-section (Which is dominant, but not to the exclusion of other terms; see Section II C),

$$\sigma_{ij}^{s-only} = |U_{\tau i}|^2 |U_{\tau j}|^2 \frac{|g|^4}{16\pi} \frac{s}{(s - M_\phi^2)^2 + M_\phi^2 \Gamma^2} , \qquad (3)$$

where $s \equiv 2E_\nu m_j$ is the center-of-momentum energy squared and m_j is the mass of ν_j. Since $U_{\tau i} \sim \mathcal{O}(1)$ for all mass eigenstates, the astrophysical spectrum will generically feature multiple absorption dips, located at $E_\nu \sim M_\phi^2/(2m_j)$ with $j \in \{1, 2, 3\}$, where the cross-section is resonantly enhanced [48, 62, 63].

The separation between these dips, and thus their separate observability, depends on the neutrino mass spectrum. In the last few years, there has been a lot of progress in understanding it: cosmological data bounds the total neutrino mass $\sum m_\nu < 0.12\,\mathrm{eV}$ at 95% CL [23], and neutrino oscillation data prefer the Normal mass Ordering (NO), i.e., $m_3 > m_2 > m_1$, over the Inverted mass Ordering (IO), i.e., $m_2 > m_1 > m_3$, with $\sim 2.5\sigma$ [40]. Admittedly, the cosmological bound is subject to some model-dependence [64–66], and the oscillation preference has lately weakened [40]. However, both hints are already statistically significant and the situation should improve quickly. For simplicity, we calculate our results assuming the NO. As we show below, the main difference between the NO and the IO appears in present IceCube data,
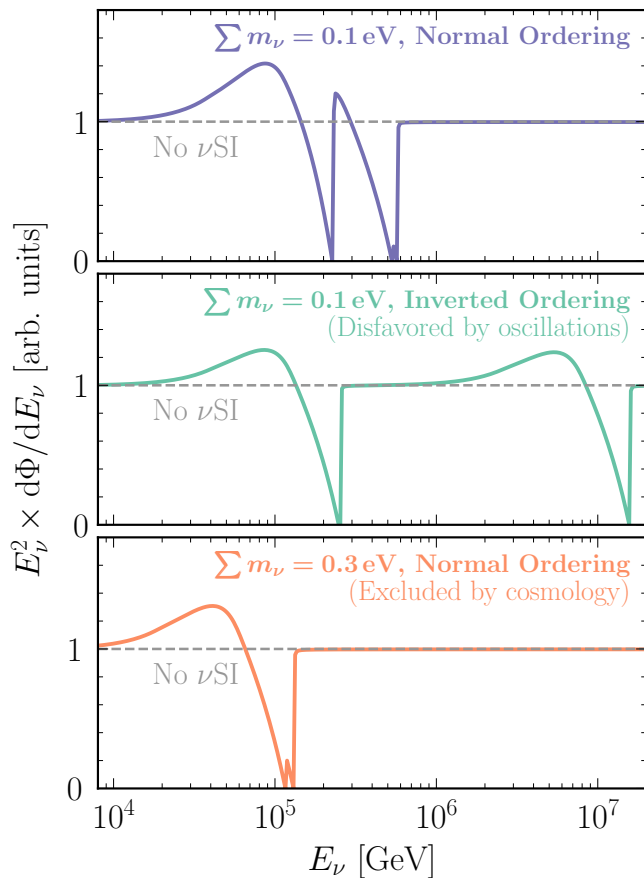
FIG. 2: Neutrino flux at Earth assuming an astrophysical flux $\propto E_\nu^{-2}$ and ν_τ self-interactions ($g = 0.01$ and $M_\phi = 5\,\text{MeV}$), for different neutrino mass scenarios. *The scenario in the top panel, favored at $\gtrsim 2.5\sigma$ over the other two scenarios, would produce two close dips in the astrophysical neutrino spectrum.*

which is not our focus. For Gen2, we show that it has comparable sensitivity to νSI for both mass orderings.

In the NO, νSI in the ν_τ sector should feature *two* absorption dips, separated in energy by an $\mathcal{O}(1)$ factor. The reason for this is as follows. First, $\sum m_\nu < 0.12\,\text{eV}$, together with the measured neutrino squared mass splittings $\sqrt{|\Delta m_{32}^2|} \sim \sqrt{|\Delta m_{31}^2|} \sim 0.05\,\text{eV}$, implies that the mass eigenstates are not degenerate. At the same time, for the NO the spectrum contains one heavy state and two light states (as $|\Delta m_{31}^2| \gg \Delta m_{21}^2$, i.e., $m_3 \gg m_1 \sim m_2$); whereas for the IO there are two heavy states and one light state ($m_2 \sim m_1 \gg m_3$). Thus, for the same total neutrino mass, the lightest mass for the NO (m_1) will typically be much larger than the lightest mass for the IO (m_3). As a consequence, the NO will generically imply that light and heavy mass eigenstates are closer to each other, i.e., for the NO the νSI absorption dips will be closer to each other.

Figure 2 shows these features. We display the all-flavor high-energy astrophysical neutrino flux at Earth obtained by numerically solving Eq. (2). We plot this as $E_\nu^2\, d\phi/dE_\nu \simeq 2.3^{-1}\, E_\nu\, d\phi/d\log_{10} E_\nu$, so that the con-
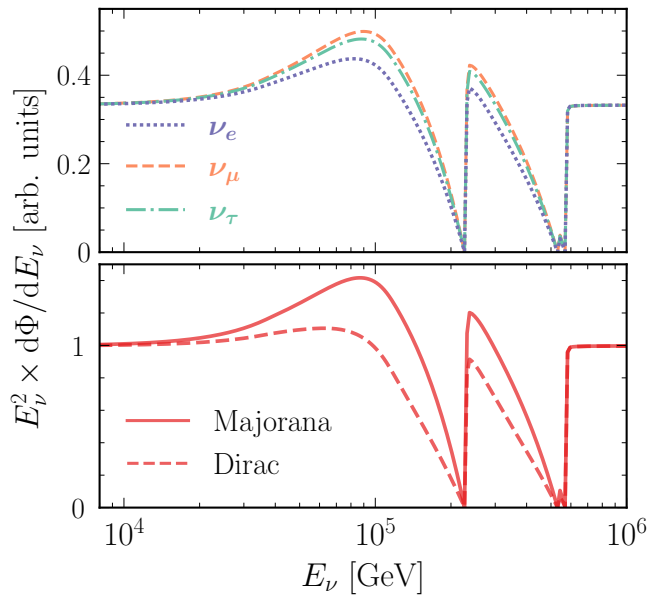

FIG. 3: Subleading effects in the neutrino flux at Earth , assuming an astrophysical flux $\propto E_\nu^{-2}$ and ν_τ self-interactions ($g = 0.01$ and $M_\phi = 5\,\text{MeV}$), **Top**: Flux for each neutrino flavor, assuming equal production of all mass eigenstates. Within the relevant precision and focusing on the dips, *observing the all-flavor flux is enough to explore ν_τ self-interactions.* **Bottom**: All-flavor flux, contrasting Majorana neutrinos [solid], for which all scattering products are observable; and Dirac neutrinos [dashed], for which some scattering products are sterile.

served area under each curve represents the conservation of energy (for the Majorana case, as discussed below). We observe the two dips due to neutrino absorption, as well as the bumps due to the scattering products moving to lower energies. Although absorption mostly takes place at $E_\nu = M_\phi^2/(2m_j)$, neutrino energy gets redshifted as the Universe expands, extending the dips to lower energies. While the IO also predicts two absorption dips for $\sum m_\nu = 0.1\,\text{eV}$, they are separated by about two orders of magnitude in neutrino energy. As the present IceCube data covers a rather narrow energy range, this would appear as a *single* dip in the spectrum. Future neutrino telescopes as Gen2 (see Section III) should have a wider energy range and thus νSI could feature two dips even for the IO.

The fact that we are considering interactions only in the ν_τ sector could have an imprint on the flavor composition of the observed high-energy astrophysical neutrino flux. However, we find the effects to be modest, as shown next. The Dirac or Majorana nature of neutrinos may also affect the results. If neutrinos are Dirac fermions, part of the final scattering states could be unobservable. As a consequence, the characteristic νSI bumps will be smaller. This distinction between Dirac and Majorana neutrinos is expected in any new physics scenario where neutrinos have non-chiral interactions [67].

Figure 3 (top) shows that measuring the all-flavor flux

is enough to explore the flavor-dependent νSI we consider. We show the high-energy astrophysical neutrino flux at Earth for each neutrino flavor, obtained by numerically solving Eq. (2) for $\sum m_\nu = 0.1\,\mathrm{eV}$ and the NO. Assuming ν_τ self-interactions implies that the scattering products will be τ neutrinos, but since $U_{\tau i} \sim \mathcal{O}(1)$ for all flavors, these will quickly oscillate to an almost flavor-universal composition at Earth. A very good experimental flavor-discrimination, though, might be advantageous in the future as a signature of flavor-dependent νSI [68].

Figure 3 (bottom) shows the difference between Dirac and Majorana neutrinos. We assume the same physics parameters as in Fig. 3 (top), but by requiring neutrinos to be Dirac fermions, we observe smaller appearance bumps. This effect can be understood from Eqs. (1) and (3): if scattering is mediated through the s-channel resonance, it can be understood as on-shell production of ϕ followed by its decay. From Eq. (1), we see that the decay products must have opposite chiralities, and so for Dirac neutrinos one of them will be sterile. Since this effect is subleading and, furthermore, constraints on Dirac neutrino self-interactions are rather strong [6], we assume Majorana neutrinos for the rest of this work.

In short, our precise understanding of neutrino properties clearly identifies the experimental signatures we must look for to make the most of the opportunity suggested by Fig. 1 and explore tau neutrino self-interactions: multiple dips in the astrophysical spectrum with an almost flavor-independent flavor composition.

C. Importance of the Cross-Section Calculation

In Eq. (2), the neutrino self-interaction cross-section σ parametrizes all the necessary particle physics input. Here we show that approximations made in the literature were unjustified in some important cases. So far in the literature, only the s-channel contribution (Eq. (3)) has been taken into account [38, 57–59]. Furthermore, as Eq. (2) can be computationally expensive to solve, Eq. (3) was recently approximated [17, 58, 59] with a δ-function at $s = M_\phi^2$.

Figure 4 shows that other contributions to the cross-section (see Appendix A) are in fact dominant for $s > M_\phi^2$. One can check that for coupling strengths $g \sim O(0.1)$— according to Fig. 1, the couplings that impact our understanding of the early universe — the astrophysical neutrino interaction probability is large even for $s > M_\phi^2$, and so other scattering channels must be taken into account.

Figure 5 shows that these other scattering channels are quantitatively important. We show the all-flavor high-energy astrophysical neutrino flux at Earth, obtained by numerically solving Eq. (2) under different approximations for different lines; in all cases we assume $\sum m_\nu = 0.1\,\mathrm{eV}$ and the NO. As we see, for coupling strengths $\mathcal{O}(0.1)$, all contributions to the cross-section must be included to correctly predict the neutrino spec-
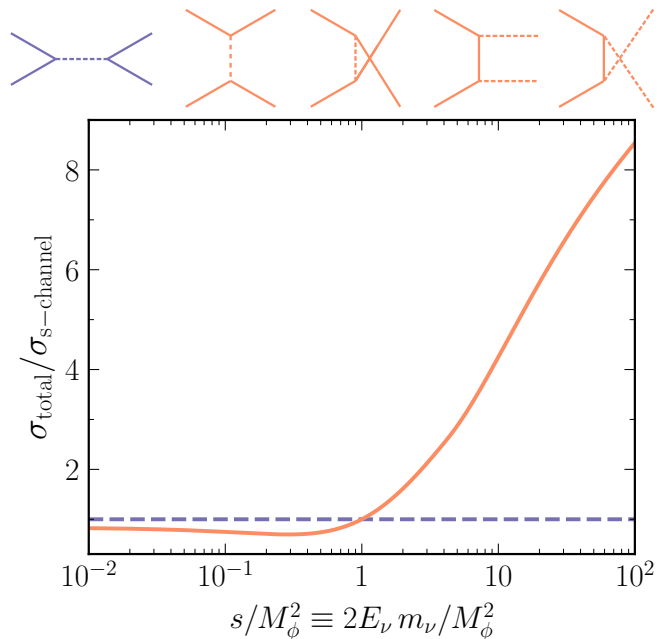

FIG. 4: Comparison of the s-channel cross-section with other contributions. **Top**: All diagrams that contribute to neutrino-neutrino scattering at lowest order. For double-scalar production, the scalars quickly decay to neutrinos. **Bottom**: Total neutrino self-interaction cross-section divided by the s-channel contribution as a function of the scaled center-of-momentum energy squared. *At high energies, the s-channel contribution is subdominant.*

trum, and the δ-function approximation is unreliable. For $g \sim 0.01$, on the other hand, all approximations are quantitatively justified. Notice that, for $g = 0.1$, the error introduced by only including s-channel scattering is smaller than the naive expectation from Fig. 4. This is because, for non s-channel scattering, the final-state neutrinos tend to have energies relatively close to the initial neutrino, and so regeneration partially compensates absorption.

We also show that the δ-function approximation, i.e., only taking into account the scattering cross-section exactly at the resonance, gives the same result for both couplings ($g = 0.01$ and $g = 0.1$) in Fig. 5. This can be understood from the neutrino mean free path at the resonance, which, ignoring the expansion of the Universe, is [58]

$$\lambda_{\mathrm{res}} \simeq \left(n^t \sigma_{\mathrm{res}}\right)^{-1} = \left(n^t \pi |U_{\tau i}|^2 \frac{g^2}{M_\phi^2}\right)^{-1}$$
$$\sim \mathrm{kpc} \times g^{-2} \left(\frac{0.1}{|U_{\tau i}|^2}\right) \left(\frac{M_\phi}{5\,\mathrm{MeV}}\right)^2, \tag{4}$$

which is much smaller than the typical distances to astrophysical sources, $\sim 1/H_0 \sim \mathrm{Gpc}$, as long as $g \gtrsim 10^{-3}$ (notice that oscillation data imply $|U_{\tau i}| \neq 1$ [40–42]). That is — assuming mediator masses $\mathcal{O}(1$–$10\,\mathrm{MeV})$ — for all couplings $g \gtrsim 10^{-3}$ all astrophysical neutrinos will be scattered at $E = E_{\mathrm{res}}$ regardless of g, and so the δ-function approximation will always give the same result.
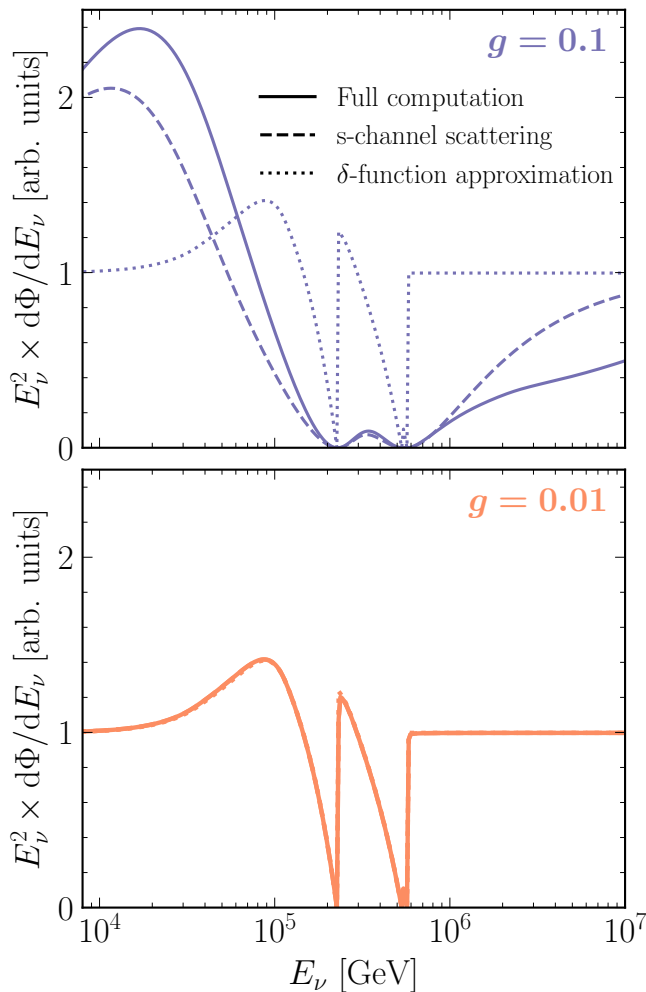
FIG. 5: Neutrino flux at Earth in the presence of νSI, using different approximation levels to solve Eq. (2). We assume an astrophysical flux $\propto E_\nu^{-2}$ and ν_τ self-interactions ($M_\phi = 5\,\mathrm{MeV}$). **Top**: For $g = 0.1$, a full calculation is needed to obtain correct results. **Bottom**: For $g = 0.01$, approximations may be made. *To cover the full space of allowed and cosmologically relevant νSI, a full calculation is needed.*

This highlights the importance of carrying out the full theoretical calculation to obtain reliable results.

Figure 6 (top) shows that the effects discussed above are also present after including detection effects. We show in the top panel the expected number of events at IceCube in each bin of deposited energy in the detector, E_{dep}. (Note that here we plot the number of events per log bin, not the energy-weighted version of that, so now the spectrum is falling.) To simulate the detector response, we use the official high-energy starting event (HESE) data release [44]. We adjust the normalization to predict 10 events in the lowest energy bin as approximately observed by IceCube (see Section III A), and for νSI we assume $\sum m_\nu = 0.1\,\mathrm{eV}$ and the NO. We can see the *two* distinct dips, appearing at $E_{\mathrm{dep}} \sim 2.5 \times 10^5\,\mathrm{GeV}$ and $E_{\mathrm{dep}} \sim 5.5 \times 10^5\,\mathrm{GeV}$ in the presence of νSI. The effect of the appearance bump is that, for
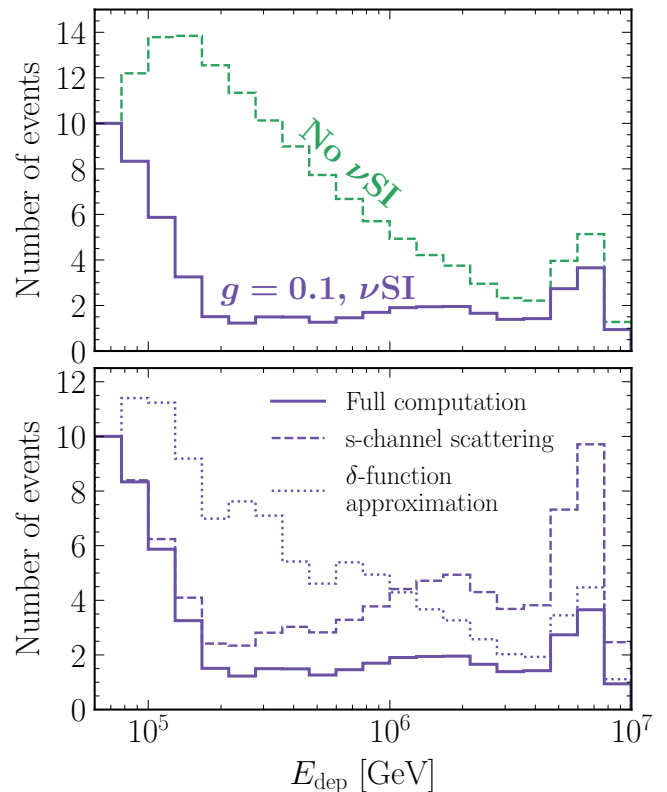

FIG. 6: Astrophysical neutrino events at Earth as a function of deposited energy in the detector E_{dep}, assuming a neutrino flux $\propto E_\nu^{-2}$. For the νSI scenario, we assume $g = 0.1$ and $M_\phi = 5\,\mathrm{MeV}$. **Top**: Spectrum with and without νSI. *νSI leads to quantitatively relevant multiple dips and bumps in the detector.* **Bottom**: νSI spectrum obtained by using different approximations to solve Eq. (2). *Unjustified approximations lead to incorrect experimental predictions.*

$E_{\mathrm{dep}} < 2 \times 10^5\,\mathrm{GeV}$, the neutrino spectrum is steeper than without νSI. From here, we already foresee a degeneracy between νSI and the spectral index. Breaking it will require observing the spectrum at a wide neutrino energy range.

The bump at $E_{\mathrm{dep}} \sim 6 \times 10^6\,\mathrm{GeV}$ is the Glashow resonance [69], i.e., resonant production of a W boson in neutrino-electron scattering. This feature has been recently observed by IceCube [70] and provides a window to the high-energy spectrum. As shown in Section III, this can help in exploring νSI.

Figure 6 (bottom) shows that, for couplings $g \sim 0.1$, not including the full cross-section largely overestimates the number of events. We show there the same high-energy astrophysical neutrino flux in the presence of νSI as in the top panel, but for different levels of approximation when solving Eq. (2). Such approximations were mostly used to speed up the computations. In our numerical code they are largely unnecessary, as it has been optimized to have a low computational cost. As we make the code publicly available, it can be easily employed in further studies.
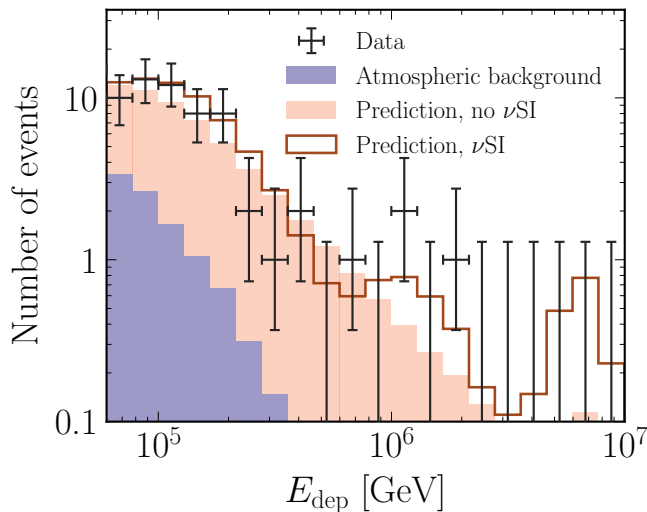
FIG. 7: HESE 7.5-year data as a function of the deposited energy. The shaded histograms show the best-fit expectations with no new physics for the atmospheric background and the astrophysical neutrino signal ($\propto E_\nu^{-2.87}$). *The data can also be accommodated by νSI with $g = 0.1$, $M_\phi = 7.5\,\mathrm{MeV}$, $\sum m_\nu = 0.07\,\mathrm{eV}$, the NO, and a modified astrophysical spectrum ($\propto E_\nu^{-2}$) [solid red line].* The large allowed coupling requires taking into account the effects discussed in Section II C.

III. ICECUBE-GEN2: THE ROAD TO PRECISION NEUTRINO ASTROPHYSICS

In this section, we show that Gen2 will be a unprecedented tool for probing νSI. In Section III A, we review the present IceCube data and discuss its limitations for exploring νSI. In Section III B, we discuss how these limitations will be overcome by Gen2. Finally, in Section III C, we carry out a data analysis to quantify the future sensitivity of Gen2 to νSI as well as the present exclusion by IceCube.

A. Status of IceCube Data

The IceCube observatory has firmly established the existence of high-energy astrophysical neutrinos by detecting $\mathcal{O}(100)$ neutrinos with $\mathcal{O}(0.1-1)$ PeV energies. As νSI introduce an energy-dependent distortion in the astrophysical neutrino spectrum, probing them requires a good reconstruction of the neutrino energy. The HESE dataset [71] is particularly appropriate for this, as it only includes neutrinos interacting within the internal part of the detector, thus reducing the amount of energy deposited outside the instrumented volume.

Figure 7 shows that, intriguingly, the IceCube HESE data suggests some non-trivial spectral features. High-energy astrophysical acceleration mechanisms generically predict that the neutrino spectrum should follow a power law as a function of energy [72, 73]. This would roughly correspond to a straight line in Fig. 7, but the data shows
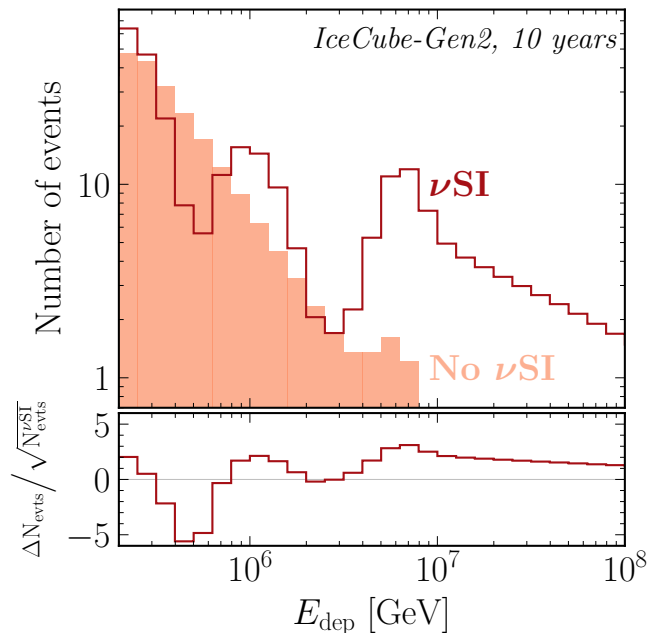

FIG. 8: Spectra for the same parameters as Fig. 7, but now projecting for Gen2 (note the change in energy range), which turns small differences into large ones. *The increased statistics and the wider energy range reduce the degeneracy with the unknown astrophysical flux (here $\propto E_\nu^{-2}$ for νSI and $\propto E_\nu^{-2.87}$ for no νSI), dramatically increasing the sensitivity to νSI.*

some deviations. In particular, there seems to be a deficit of events at $E_{\mathrm{dep}} \sim 5 \times 10^5$ GeV, and an excess at $E_{\mathrm{dep}} \sim 10^6$ GeV. These features have been interpreted in the literature as hints for νSI [17, 57, 59].

To illustrate this point, we show in Fig. 7 that the spectrum can be fit by nonzero νSI and a different spectral index. While the fit is visually better than the no-νSI case, we caution that the significance is not high (see Section III C). This νSI interpretation relies on the presence of *two* separate dips (at $E_{\mathrm{dep}} \sim 5 \times 10^5$ GeV and at $E_{\mathrm{dep}} \sim 3 \times 10^6$ GeV), each with its corresponding bump at lower energies. We also note that the degeneracy between νSI parameters and the spectral index could perhaps be exploited to reduce the longstanding tension in the different values of the spectral index deduced from different IceCube datasets [71, 74, 75]. However, this is beyond our scope.

This discussion identifies two weaknesses of the present IceCube data to explore νSI: apart from having relatively low statistics, the data only covers about one order of magnitude in neutrino energy. As Figs. 2 to 6 show, νSI-induced spectral features cover a wide energy range. Furthermore, a wider energy coverage also entails a better understanding of the spectral index that to some extent can be degenerate with νSI-induced dips, as Fig. 7 shows.

B. Prospects for Gen2

Fortunately, Gen2 [45] will overcome the issues noted above for IceCube. Its effective volume will be about one order of magnitude larger, so Fig. 7 already indicates that Gen2 should observe events up to, at least, energies $E_{\rm dep} \sim 10^7$ GeV.

To quantify the potential of this future observatory, we carry out a simplified but realistic simulation of Gen2. We take the Gen2 optical effective area from Fig. 25 in Ref. [45], and compute the deposited energy distribution following Refs. [76, 77]. We assume an energy resolution of 10% for the deposited energy. Following Ref. [45], we assume a minimum detectable neutrino energy of 200 TeV, below which the data may contain too many atmospheric background events.

Figure 8 shows that Gen2 will indeed be very sensitive to νSI. We show the expected numbers of events after 10 years of data taking as a function of deposited energy, using the same physics parameters as in Fig. 7 (When comparing with Fig. 7, notice also that here the energy range is wider and we show 10 bins per decade instead of 9.) The bottom panel shows the difference between the expected number of events with and without νSI, divided by the square root of the former, which gives a conservative unverestimate of the expected statistical uncertainties. As we see, unlike presently at IceCube, the much wider energy range together with the increased statistics will undoubtedly disentangle a power-law spectrum from νSI with a modified spectral index. To better understand the sensitivity of Gen2, though, we must explore the impact of weaker νSI.

Figure 9 quantitatively shows that even relatively weak νSI would profoundly impact the Gen2 observations. We show the expected spectrum in Gen2, assuming a normalization compatible with current IceCube observations. In the bottom panel, we show the difference between the number of events with and without νSI, divided by the expected statistical uncertainties.

The dotted purple line is of particular physical relevance. It corresponds to the coupling at which, for $M_\phi = 10$ MeV, the neutrino mean free path (c.f. Eq. (4)) is 1 Gpc, roughly the distance to astrophysical neutrino sources. We expect the effects shown by that line to be close to the largest νSI propagation effects at any neutrino telescope: for smaller couplings, the observable neutrino flux attenuation, $\sim e^{-g^2/M_\phi^2}$, is exponentially small. According to the bottom panel, Gen2 should have enough statistical power to be sensitive to the dotted purple line. It will thus realize the full potential of high-energy astrophysical neutrino propagation for testing νSI.

The results above also illustrate that the unique spectral features cannot be accommodated by a modified power law and so would be a smoking gun for νSI. Notice that it is not easy for random statistical fluctuations to emulate νSI, because (1) the separation between the absorption dips is precisely determined by external neutrino oscillation and cosmological data, and (2) νSI predict a
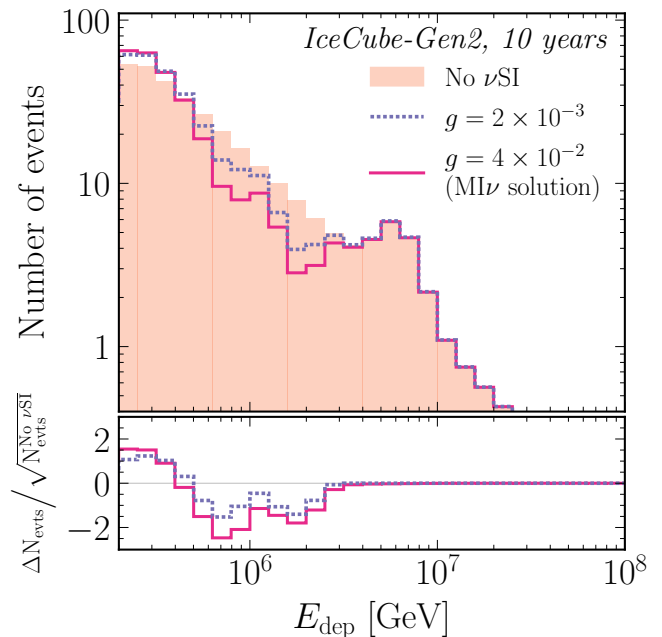

FIG. 9: Expected spectrum of astrophysical neutrino events in Gen2, showing the sensitivity to small couplings. In all cases, the assumed astrophysical spectrum is $\propto E_\nu^{-2.5}$. The solid line corresponds to the MIν solution for $M_\phi = 10$ MeV, showing that *cosmologically-relevant νSI would imprint significant features in the Gen2 spectrum.* The dotted line corresponds to the limiting sensitivity of Gen2, *which cannot be significantly improved upon with neutrino telescopes (see text).*

bump with a fixed amplitude just below the lowest energy dip. These features suggest that, should spectral anomalies appear at Gen2, it could be relatively easy to identify them as being due to νSI or not.

C. νSI sensitivity

To quantify the future sensitivity of Gen2, along with the νSI presently allowed by IceCube, we carry out a data analysis using the theoretical framework discussed in Section II.

Starting with the present IceCube HESE data, we follow the procedure in the official data release [71, 78]. We assume an initial neutrino flux following a power law with spectral index $\gamma \in [2,3]$ and an all-neutrino normalization at $E_\nu = 100$ TeV $\phi_{6\nu}(100\,{\rm TeV}) \in [10^{-16}, 10^{-20}]\,{\rm GeV}^{-1}\,{\rm cm}^{-2}\,{\rm s}^{-1}\,{\rm sr}^{-1}$. In addition to the standard analysis parameters, we include ν_τ self-interactions parametrized by the coupling strength g, the mediator mass M_ϕ, and the total neutrino mass $\sum m_\nu$. For $\sum m_\nu$, we include as a prior the cosmological bound coming from CMB and Baryon Acoustic Oscillation data [23], $\sum m_\nu < 0.12$ eV (95% CL). We assume the NO and the neutrino squared mass splittings and mixings from Ref. [40].

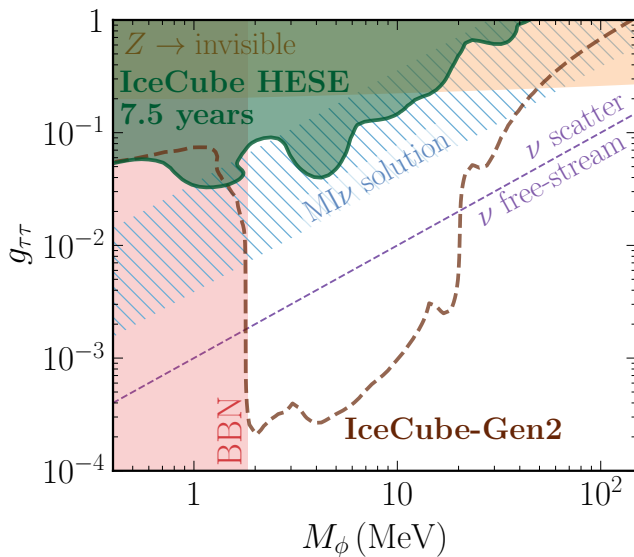To forecast the expected sensitivity of Gen2, we gener-

FIG. 10: Present and future sensitivity to ν_τ self-interactions, along with present bounds and cosmologically relevant regions (c.f. Fig. 1). The dark green region, including part of the MIν region, is excluded by IceCube data, and the dashed brown line shows the Gen2 sensitivity (2σ). *Gen2 will exploit the full potential of testing νSI with high-energy astrophysical neutrino propagation* (see text), *being sensitive to a large parameter space where neutrinos have a non-trivial cosmological behavior.* Comparable constraints would apply to other flavors too.

ate mock data corresponding to 10 years of exposure at Gen2, together with 15 years of IceCube exposure for deposited energies $E_{\rm dep} \in [6 \times 10^4, 2 \times 10^5]\,{\rm GeV}$ that are below the range of Gen2 [45]. We assume an all-neutrino astrophysical flux following a power law, $\phi_{6\nu}(E_\nu) = 5 \times 10^{-18}(E_\nu/100\,{\rm TeV})^{-2.5}\,{\rm GeV}^{-1}\,{\rm cm}^{-2}\,{\rm s}^{-1}\,{\rm sr}^{-1}$, compatible with present IceCube data (the particular power law is not important; see below). We analyze the mock data assuming νSI as outlined in the paragraph above (including marginalizing over the spectral index when assuming νSI). By the time Gen2 goes online, we expect a precise cosmological determination of $\sum m_\nu$ [32–36], so we fix this to 0.1 eV. We use only the HESE spectrum, and do not exploit flavor information.

Figure 10 shows that Gen2 will have a superb sensitivity, covering a huge range of cosmologically relevant νSI parameters. The shape of the Gen2 sensitivity curve can be easily understood. Its largest sensitivity to the coupling strength g covers about one order of magnitude in M_ϕ which, for resonant scattering (i.e., $M_\phi^2 \sim 2E_\nu m_\nu$) corresponds to two orders of magnitude in neutrino energy. As we see from Fig. 8, this is roughly the energy range of Gen2.

The abrupt sensitivity decrease for $M_\phi < 2\,{\rm MeV}$ is because, at these mediator masses and for $\sum m_\nu = 0.1\,{\rm eV}$, the highest-energy νSI resonant absorption dip is below the smallest detectable energy. Gen2 will only be sensitive to such small mediator masses if neutrino-neutrino

scattering outside the resonance is relevant. This, as Fig. 5 shows, only happens for coupling strengths $g \sim 0.1$. These results also illustrate that, since the low-energy statistics is very large (c.f. Fig. 9), the presence of a single spectral feature is enough to probe νSI. This implies similar sensitivity to the NO and the IO (c.f. Fig. 2).

For $2\,{\rm MeV} \lesssim M_\phi \lesssim 20\,{\rm MeV}$, the Gen2 sensitivity can be approximated as $g/M_\phi \sim$ few times $10^{-4}\,{\rm MeV}^{-1}$. This corresponds to a neutrino mean free path at the resonance (c.f. Eq. (4)) $\lambda_{\rm res} \sim {\rm Gpc} \sim H_0^{-1}$, the typical distance to astrophysical neutrino sources. As, for lower couplings, the observable neutrino flux attenuation decreases exponentially, $\sim e^{-g^2/M_\phi^2}$, it would be very challenging to get beyond this sensitivity with high-energy astrophysical neutrino propagation effects.

There are also some local sensitivity improvements for mediator masses of $\sim 4\,{\rm MeV}$, $\sim 20\,{\rm MeV}$, and $\sim 30\,{\rm MeV}$: the first corresponds to the mediator mass at which the second absorption dip is above the smallest detectable energy; and the last two are due to νSI spectral features having the same energy as the Glashow resonance, which increases their statistics. The sensitivity decreases again for $M_\phi \gtrsim 20\,{\rm MeV}$, the mediator masses above which the highest-energy νSI dip is at energies $E_{\rm dep} \gtrsim 10^7\,{\rm GeV}$. Although there are still other νSI features in the spectrum, the poor statistics at high energies dramatically reduces the sensitivity. Notice that this particular mediator mass above which Gen2 loses sensitivity depends on the spectral index, which sets the highest energy neutrinos that can be detected: we have checked that changing the spectral index to 2.0 or 3.0 only changes the higher end of the Gen2 sensitivity by about a factor of 2 in M_ϕ. The other aspects of the Gen2 sensitivity line are insensitive to the assumed spectral index.

Fig. 10 also shows the present IceCube HESE exclusion region. It is more powerful than BBN and Z decay bounds in some regions of the νSI parameter space, and complementary in others. Furthermore, it is powerful enough to exclude the MIν solution for mediator masses $1\,{\rm MeV} \lesssim M_\phi \lesssim 10\,{\rm MeV}$ and coupling strengths $g \gtrsim 0.05$. The explored coupling range already indicates the relevance of the theoretical effects we discuss in Section II: we have checked that, if we ignored them, the excluded region would be quantitatively different.

Finally, let us notice that, unlike previous works [17, 57, 59], we do not find any statistically significant indication in favor of νSI in present IceCube data. In particular, despite being described by more parameters, νSI are only preferred over a simple power law neutrino spectrum at the $\sim 1\sigma$ level. This difference may stem from our more precise theoretical treatment described in Section II, our use of a more recent data set, our precise treatment of detector effects that matches that used by the experimental collaboration, or a combination of these effects.

Both Figs. 9 and 10 illustrate that Gen2 will be a very powerful tool to explore νSI. We expect it to be sensitive to the full range of the presently allowed MIν so-

lution and to almost all allowed interaction models for which cosmological neutrinos do not free-stream. The remaining allowed region where cosmological neutrinos do not free-stream could be explored with higher-energy observatories including Gen2-radio [45, 79–83]. Furthermore, for mediator masses between 2 and 20 MeV, Gen2 would realize the full potential of neutrino astronomy to test νSI, even competing with the strongest laboratory probes (see meson-decay limits in Fig. 1) and setting the strongest bound on νSI. Since the presence of a single spectral feature is enough to probe νSI at Gen2, we expect the constraints from Fig. 10 to apply with comparable strength to ν_e and ν_μ. This future observatory will thus be a unique bridge between the cosmological and laboratory quests to understand if neutrinos have large self-interactions.

IV. CONCLUSIONS AND OUTLOOK

We return to our opening question: Do neutrinos have sizable self-interactions? In the laboratory, this is impossible to answer through scattering and is not adequately constrained through particle decays. But this question is of central importance to particle theory, as neutrinos allow unique tests of new physics. And it is of central importance to cosmology, as allowed νSI parameters would indicate the presence of strong self-scattering in the early universe. New techniques to probe νSI are needed, especially in the ν_τ sector. These may lead to discoveries that should be tested in multiple ways, or to limits that will improve our abilities to search for physics beyond the standard models of particle physics and cosmology.

A way forward is to look for signatures of scattering with neutrinos in the CνB, which leads to characteristic features in the spectrum of astrophysical neutrinos at Earth [37–39]. This has become newly promising now that IceCube has detected $\mathcal{O}(100)$ events at energies larger than 60 TeV [43, 44].

In this paper, we take advantage of the proposed Gen2 detector, develop a comprehensive theoretical treatment, and make predictions that include realistic experimental effects. We benefit from the improved knowledge of the neutrino mass spectrum: the measurements of the total neutrino mass in cosmology and of the neutrino mass ordering in the laboratory shape the experimental signatures that should be looked for. We also demonstrate that common approximations in the literature were unjustified in some important cases.

Our primary result is that Gen2 will significantly improve the sensitivity to νSI, realizing the full potential of high-energy neutrino astronomy for testing νSI in propagation. It can probe a huge range of parameters where neutrinos do not free-stream as expected in the early universe. This includes the full parameter space relevant for the Moderately Interacting neutrino solution [6, 25]. At its best sensitivity — for mediator masses $2\,\mathrm{MeV} \lesssim M_\phi \lesssim 20\,\mathrm{MeV}$ —, it will overcome laboratory

constraints and become the strongest probe of neutrino self-interactions *between any flavors*. The future quest for νSI discovery will not remain bounded to τ neutrinos as it is today.

As we make our code publicly available, the same formalism can be straightforwardly applied to explore different parts of the parameter space with various sources. Some examples include the diffuse supernova neutrino background or cosmogenic neutrinos. Exploring non-propagation effects (see, e.g., Ref. [18]) could be complementary.

In this work, we only exploit the signatures in the Gen2 diffuse spectrum, being agnostic about the underlying astrophysical flux and its flavor composition. Any improvement in understanding the energy-dependent flavor sensitivity of Gen2 could provide additional constraints (Ref. [68] already demonstrates the superb flavor discrimination of Gen2 and other future high-energy neutrino detectors). In connection to this, we derive sensitivities using a simplified simulation of Gen2 that should nevertheless capture the main effects. Developments in detector simulation or taking into account potential statistical fluctuations of the data would help to sharpen our understanding of the potential of Gen2.

Should a signal appear, there will be plenty of opportunities to test it. The main purpose of Gen2 is to resolve individual neutrino sources [45]; any detection would be highly valuable to explore νSI [84]. The reason is that nearby sources should not be affected by νSI and could provide a better understanding of the high-energy astrophysical neutrino spectrum. The appearance of spectral signatures in far but not near sources would be a smoking gun for νSI.

Furthermore, the scattering of neutrinos en route to the Earth could "blur" point sources and introduce time delays [38]. The angular deflections, $\mathcal{O}(10^{-8})$, are in principle negligible. In turn, the time delays $\mathcal{O}(10\,\mathrm{s})$ (or larger if neutrinos scatter several times) can be comparable to the duration of astrophysical transients [45]. This would introduce interesting time-dependent effects that could be a window to better characterize νSI. If the accumulated time delays are large enough, the characteristic νSI bump could even be absent, similar to the Dirac neutrino scenario (c.f. Fig. 3).

As discussed in the text, if different IceCube datasets keep pointing towards different spectral indices, νSI could alleviate this tension by allowing for different underlying astrophysical fluxes. Such degeneracies could be disentangled with Gen2.

Finally, hints for νSI at Gen2 could leave signatures in cosmological observables. Conversely, as cosmological data gets more precise, any cosmology hint should be testable at Gen2. Although Fig. 10 shows that there is still a region of νSI beyond the Gen2 sensitivity where neutrinos do not free-stream in the early universe, ultra-high energy neutrino observatories [45, 79–83] should be sensitive to it. The improved theoretical treatment we introduce in this work, together with our public code,

should aid in exploring it.

As neutrino physics enters the precision era, the properties of these ghostly particles will be scrutinized better than ever. In this paper, we provide the necessary particle physics framework as well as the phenomenological roadmap to make the most out of neutrino self-interaction measurements in present and next-generation neutrino telescopes. Improvements in the understanding of high-energy astrophysical sources and further experimental sensitivity studies will enhance this progress. This will open a window into understanding whether neutrinos have sizable self-interactions, providing insight about physics beyond the standard model and the evolution of the early universe.

[1] K. Choi and A. Santamaria, *17-KeV neutrino in a singlet - triplet majoron model*, Phys. Lett. B **267** (1991) 504–508.

[2] A. Acker, S. Pakvasa, and J. T. Pantaleone, *Decaying Dirac neutrinos*, Phys. Rev. D **45** (1992) 1–4.

[3] A. Acker, A. Joshipura, and S. Pakvasa, *A Neutrino decay model, solar anti-neutrinos and atmospheric neutrinos*, Phys. Lett. B **285** (1992) 371–375.

[4] J. F. Beacom, N. F. Bell, and S. Dodelson, *Neutrinoless universe*, Phys. Rev. Lett. **93** (2004) 121302, [astro-ph/0404585].

[5] A. de Gouvêa, P. S. B. Dev, B. Dutta, T. Ghosh, T. Han, and Y. Zhang, *Leptonic Scalars at the LHC*, JHEP **07** (2020) 142, [1910.01132].

[6] N. Blinov, K. J. Kelly, G. Z. Krnjaic, and S. D. McDermott, *Constraining the Self-Interacting Neutrino Interpretation of the Hubble Tension*, Phys. Rev. Lett. **123** (2019), no. 19 191102, [1905.02727].

[7] B. Dasgupta and J. Kopp, *Sterile Neutrinos*, [2106.05913].

[8] J. Asaadi, E. Church, R. Guenette, B. J. P. Jones, and A. M. Szelc, *New light Higgs boson and short-baseline neutrino anomalies*, Phys. Rev. D **97** (2018), no. 7 075021, [1712.08019].

[9] B. Chauhan and S. Mohanty, *Signature of light sterile neutrinos at IceCube*, Phys. Rev. D **98** (2018), no. 8 083021, [1808.04774].

[10] A. Y. Smirnov and V. B. Valera, *Resonance refraction and neutrino oscillations*, [2106.13829].

[11] M. Dentler, I. Esteban, J. Kopp, and P. Machado, *Decaying Sterile Neutrinos and the Short Baseline Oscillation Anomalies*, Phys. Rev. D **101** (2020), no. 11 115013, [1911.01427].

[12] A. de Gouvêa, O. L. G. Peres, S. Prakash, and G. V. Stenico, *On The Decaying-Sterile Neutrino Solution to the Electron (Anti)Neutrino Appearance Anomalies*, JHEP **07** (2020) 141, [1911.01447].

[13] **Muon g-2 Collaboration**, G. W. Bennett *et al.*, *Final Report of the Muon E821 Anomalous Magnetic Moment Measurement at BNL*, Phys. Rev. D **73** (2006) 072003, [hep-ex/0602035].

[14] T. Araki, F. Kaneko, T. Ota, J. Sato, and T. Shimomura, *MeV scale leptonic force for cosmic neutrino spectrum and muon anomalous magnetic moment*, Phys. Rev. D **93** (2016), no. 1 013014, [1508.07471].

[15] S. Borsanyi *et al.*, *Leading hadronic contribution to the muon magnetic moment from lattice QCD*, Nature **593** (2021), no. 7857 51–55, [2002.12347].

[16] B. Abi *et al.*, *Measurement of the Positive Muon Anomalous Magnetic Moment to 0.46 ppm*, [2104.03281].

[17] J. A. Carpio, K. Murase, I. M. Shoemaker, and Z. Tabrizi, *High-energy cosmic neutrinos as a probe of the vector mediator scenario in light of the muon g − 2 anomaly and Hubble tension*, [2104.15136].

[18] S. Shalgar, I. Tamborra, and M. Bustamante, *Core-collapse supernovae stymie secret neutrino interactions*, Phys. Rev. D **103** (2021), no. 12 123008, [1912.09115].

[19] S. Bashinsky and U. Seljak, *Neutrino perturbations in CMB anisotropy and matter clustering*, Phys. Rev. D **69** (2004) 083002, [astro-ph/0310198].

[20] S. Hannestad, *Structure formation with strongly interacting neutrinos - Implications for the cosmological neutrino mass bound*, JCAP **02** (2005) 011, [astro-ph/0411475].

[21] S. Hannestad and G. Raffelt, *Constraining invisible neutrino decays with the cosmic microwave background*, Phys. Rev. D **72** (2005) 103514, [hep-ph/0509278].

[22] N. F. Bell, E. Pierpaoli, and K. Sigurdson, *Cosmological signatures of interacting neutrinos*, Phys. Rev. D **73** (2006) 063523, [astro-ph/0511410].

[23] **Planck Collaboration**, N. Aghanim *et al.*, *Planck 2018 results. VI. Cosmological parameters*, Astron. Astrophys. **641** (2020) A6, [1807.06209].

[24] B. D. Fields, K. A. Olive, T.-H. Yeh, and C. Young, *Big-Bang Nucleosynthesis after Planck*, JCAP **03** (2020) 010, [1912.01132]. [Erratum: JCAP 11, E02 (2020)].

[25] C. D. Kreisch, F.-Y. Cyr-Racine, and O. Doré, *Neutrino puzzle: Anomalies, interactions, and cosmological tensions*, Phys. Rev. D **101** (2020), no. 12 123505, [1902.00534].

[26] L. Verde, T. Treu, and A. G. Riess, *Tensions between the Early and the Late Universe*, Nature Astron. **3** (7, 2019) 891, [1907.10625].

[27] F.-Y. Cyr-Racine and K. Sigurdson, *Limits on Neutrino-Neutrino Scattering in the Early Universe*, Phys. Rev. D **90** (2014), no. 12 123533, [1306.1536].

[28] M. Archidiacono and S. Hannestad, *Updated constraints on non-standard neutrino interactions from Planck*, *JCAP* **07** (2014) 046, [1311.3873].

[29] L. Lancaster, F.-Y. Cyr-Racine, L. Knox, and Z. Pan, *A tale of two modes: Neutrino free-streaming in the early universe*, *JCAP* **07** (2017) 033, [1704.06657].

[30] I. M. Oldengott, T. Tram, C. Rampf, and Y. Y. Y. Wong, *Interacting neutrinos in cosmology: exact description and constraints*, *JCAP* **11** (2017) 027, [1706.02123].

[31] G.-y. Huang and W. Rodejohann, *Solving the Hubble tension without spoiling Big Bang Nucleosynthesis*, *Phys. Rev. D* **103** (2021) 123007, [2102.04280].

[32] **EUCLID Collaboration**, R. Laureijs *et al.*, *Euclid Definition Study Report*, 1110.3193.

[33] **SKA Cosmology SWG Collaboration**, R. Maartens, F. B. Abdalla, M. Jarvis, and M. G. Santos, *Overview of Cosmology with the SKA*, *PoS* **AASKA14** (2015) 016, [1501.04076].

[34] **DESI Collaboration**, A. Aghamousa *et al.*, *The DESI Experiment Part I: Science,Targeting, and Survey Design*, 1611.00036.

[35] **CMB-S4 Collaboration**, K. N. Abazajian *et al.*, *CMB-S4 Science Book, First Edition*, 1610.02743.

[36] **LSST Dark Energy Science Collaboration**, D. Alonso *et al.*, *The LSST Dark Energy Science Collaboration (DESC) Science Requirements Document*, 1809.01669.

[37] D. Hooper, *Detecting MeV Gauge Bosons with High-Energy Neutrino Telescopes*, *Phys. Rev. D* **75** (2007) 123001, [hep-ph/0701194].

[38] K. C. Y. Ng and J. F. Beacom, *Cosmic neutrino cascades from secret neutrino interactions*, *Phys. Rev. D* **90** (2014), no. 6 065035, [1404.2288]. [Erratum: Phys.Rev.D 90, 089904 (2014)].

[39] K. Ioka and K. Murase, *IceCube PeV–EeV neutrinos and secret interactions of neutrinos*, *PTEP* **2014** (2014), no. 6 061E01, [1404.2279].

[40] I. Esteban, M. C. Gonzalez-Garcia, M. Maltoni, T. Schwetz, and A. Zhou, *The fate of hints: updated global analysis of three-flavor neutrino oscillations*, *JHEP* **09** (2020) 178, [2007.14792].

[41] P. F. de Salas, D. V. Forero, S. Gariazzo, P. Martínez-Miravé, O. Mena, C. A. Ternes, M. Tórtola, and J. W. F. Valle, *2020 global reassessment of the neutrino oscillation picture*, *JHEP* **02** (2021) 071, [2006.11237].

[42] F. Capozzi, E. Di Valentino, E. Lisi, A. Marrone, A. Melchiorri, and A. Palazzo, *The unfinished fabric of the three neutrino paradigm*, 2107.00532.

[43] **IceCube Collaboration**, M. G. Aartsen *et al.*, *Characteristics of the diffuse astrophysical electron and tau neutrino flux with six years of IceCube high energy cascade data*, *Phys. Rev. Lett.* **125** (2020), no. 12 121104, [2001.09520].

[44] **IceCube Collaboration**, R. Abbasi *et al.*, *The IceCube high-energy starting event sample: Description and flux characterization with 7.5 years of data*, 2011.03545.

[45] **IceCube-Gen2 Collaboration**, M. G. Aartsen *et al.*, *IceCube-Gen2: the window to the extreme Universe*, *J. Phys. G* **48** (2021), no. 6 060501, [2008.04323].

[46] R. Laha, B. Dasgupta, and J. F. Beacom, *Constraints on New Neutrino Interactions via Light Abelian Vector Bosons*, *Phys. Rev. D* **89** (2014), no. 9 093025, [1304.3460].

[47] S. G. Karshenboim, D. McKeen, and M. Pospelov, *Constraints on muon-specific dark forces*, *Phys. Rev. D* **90** (2014), no. 7 073004, [1401.6154]. [Addendum: Phys.Rev.D 90, 079905 (2014)].

[48] K. Blum, A. Hook, and K. Murase, *High energy neutrino telescopes as a probe of the neutrino mass mechanism*, 1408.3799.

[49] J. M. Berryman, A. De Gouvêa, K. J. Kelly, and Y. Zhang, *Lepton-Number-Charged Scalars and Neutrino Beamstrahlung*, *Phys. Rev. D* **97** (2018), no. 7 075030, [1802.00009].

[50] K. J. Kelly, M. Sen, W. Tangarife, and Y. Zhang, *Origin of sterile neutrino dark matter via secret neutrino interactions with vector bosons*, *Phys. Rev. D* **101** (2020), no. 11 115031, [2005.03681].

[51] V. Brdar, M. Lindner, S. Vogl, and X.-J. Xu, *Revisiting neutrino self-interaction constraints from Z and τ decays*, *Phys. Rev. D* **101** (2020), no. 11 115001, [2003.05339].

[52] K. J. Kelly and Y. Zhang, *Mononeutrino at DUNE: New Signals from Neutrinophilic Thermal Dark Matter*, *Phys. Rev. D* **99** (2019), no. 5 055034, [1901.01259].

[53] A. Arbey, *AlterBBN: A program for calculating the BBN abundances of the elements in alternative cosmologies*, *Comput. Phys. Commun.* **183** (2012) 1822–1831, [1106.1363].

[54] A. Arbey, J. Auffinger, K. P. Hickerson, and E. S. Jenssen, *AlterBBN v2: A public code for calculating Big-Bang nucleosynthesis constraints in alternative cosmologies*, *Comput. Phys. Commun.* **248** (2020) 106982, [1806.11095].

[55] T. Weiler, *Resonant absorption of cosmic-ray neutrinos by the relic-neutrino background*, *Phys. Rev. Lett.* **49** (Jul, 1982) 234–237.

[56] E. Roulet, *Ultrahigh energy neutrino absorption by neutrino dark matter*, *Phys. Rev. D* **47** (Jun, 1993) 5247–5252.

[57] M. Bustamante, C. Rosenstrøm, S. Shalgar, and I. Tamborra, *Bounds on secret neutrino interactions from high-energy astrophysical neutrinos*, *Phys. Rev. D* **101** (2020), no. 12 123024, [2001.04994].

[58] C. Creque-Sarbinowski, J. Hyde, and M. Kamionkowski, *Resonant neutrino self-interactions*, *Phys. Rev. D* **103** (2021), no. 2 023527, [2005.05332].

[59] A. Mazumdar, S. Mohanty, and P. Parashari, *Flavour specific neutrino self-interaction: H_0 tension and IceCube*, 2011.13685.

[60] A. M. Hopkins and J. F. Beacom, *On the normalisation of the cosmic star formation history*, *Astrophys. J.* **651** (2006) 142–154, [astro-ph/0601463].

[61] H. Yuksel, M. D. Kistler, J. F. Beacom, and A. M. Hopkins, *Revealing the High-Redshift Star Formation Rate with Gamma-Ray Bursts*, *Astrophys. J. Lett.* **683** (2008) L5–L8, [0804.4008].

[62] A. DiFranzo and D. Hooper, *Searching for MeV-Scale Gauge Bosons with IceCube*, *Phys. Rev. D* **92** (2015), no. 9 095007, [1507.03015].

[63] J. F. Cherry, A. Friedland, and I. M. Shoemaker, *Short-baseline neutrino oscillations, Planck, and IceCube*, 1605.06506.

[64] E. Di Valentino, A. Melchiorri, and J. Silk, *Cosmological constraints in extended parameter space from the Planck*

2018 Legacy release, *JCAP* **01** (2020) 013, [1908.01391].

[65] M. Escudero, J. Lopez-Pavon, N. Rius, and S. Sandner, *Relaxing Cosmological Neutrino Mass Bounds with Unstable Neutrinos*, *JHEP* **12** (2020) 119, [2007.04994].

[66] I. Esteban and J. Salvado, *Long Range Interactions in Cosmology: Implications for Neutrinos*, *JCAP* **05** (2021) 036, [2101.05804].

[67] M. Zralek, *On the possibilities of distinguishing Dirac from Majorana neutrinos*, *Acta Phys. Polon. B* **28** (1997) 2225–2257, [hep-ph/9711506].

[68] N. Song, S. W. Li, C. A. Argüelles, M. Bustamante, and A. C. Vincent, *The Future of High-Energy Astrophysical Neutrino Flavor Measurements*, *JCAP* **04** (2021) 054, [2012.12893].

[69] S. L. Glashow, *Resonant Scattering of Antineutrinos*, *Phys. Rev.* **118** (1960) 316–317.

[70] **IceCube Collaboration**, M. G. Aartsen *et al.*, *Detection of a particle shower at the Glashow resonance with IceCube*, *Nature* **591** (2021), no. 7849 220–224. [Erratum: Nature 592, E11 (2021)].

[71] **IceCube Collaboration**, R. Abbasi *et al.*, *The IceCube high-energy starting event sample: Description and flux characterization with 7.5 years of data*, 2011.03545.

[72] E. Fermi, *On the Origin of the Cosmic Radiation*, *Phys. Rev.* **75** (1949) 1169–1174.

[73] T. K. Gaisser, R. Engel, and E. Resconi, *Cosmic Rays and Particle Physics: 2nd Edition*. Cambridge University Press, 6, 2016.

[74] **IceCube Collaboration**, M. G. Aartsen *et al.*, *The IceCube Neutrino Observatory - Contributions to ICRC 2015 Part II: Atmospheric and Astrophysical Diffuse Neutrino Searches of All Flavors*, in *34th International Cosmic Ray Conference*, 10, 2015. 1510.05223.

[75] A. Palladino, C. Mascaretti, and F. Vissani, *On the compatibility of the IceCube results with a universal neutrino spectrum*, *Eur. Phys. J. C* **77** (2017), no. 10 684, [1708.02094].

[76] R. Gandhi, C. Quigg, M. H. Reno, and I. Sarcevic, *Neutrino interactions at ultrahigh-energies*, *Phys. Rev. D* **58** (1998) 093009, [hep-ph/9807264].

[77] R. Laha, J. F. Beacom, B. Dasgupta, S. Horiuchi, and K. Murase, *Demystifying the PeV Cascades in IceCube: Less (Energy) is More (Events)*, *Phys. Rev. D* **88** (2013) 043009, [1306.2309].

[78] A. Schneider, "Precision measurements of the astro-physical neutrino flux." https://raw.githubusercontent.com/austinschneider/gradthesis/master/thesis_submitted.pdf.

[79] **GRAND Collaboration**, O. Martineau-Huynh *et al.*, *The Giant Radio Array for Neutrino Detection*, *EPJ Web Conf.* **116** (2016) 03005, [1508.01919].

[80] **ARA Collaboration**, P. Allison *et al.*, *Constraints on the diffuse flux of ultrahigh energy neutrinos from four years of Askaryan Radio Array data in two stations*, *Phys. Rev. D* **102** (2020), no. 4 043021, [1912.00987].

[81] Q. Abarr *et al.*, *The Payload for Ultrahigh Energy Observations (PUEO): A White Paper*, 2010.02892.

[82] **POEMMA Collaboration**, A. V. Olinto *et al.*, *The POEMMA (Probe of Extreme Multi-Messenger Astrophysics) observatory*, *JCAP* **06** (2021) 007, [2012.07945].

[83] S. Prohira *et al.*, *The Radar Echo Telescope for Cosmic Rays: Pathfinder Experiment for a Next-Generation Neutrino Observatory*, 2104.00459.

[84] K. J. Kelly and P. A. N. Machado, *Multimessenger Astronomy and New Neutrino Physics*, *JCAP* **10** (2018) 048, [1808.02889].

[85] H. E. Haber, *Spin formalism and applications to new physics searches*, in *21st Annual SLAC Summer Institute on Particle Physics: Spin Structure in High-energy Processes (School: 26 Jul - 3 Aug, Topical Conference: 4-6 Aug) (SSI 93)*, pp. 231–272, 4, 1994. hep-ph/9405376.

[86] **Particle Data Group Collaboration**, P. Zyla *et al.*, *Review of Particle Physics*, *PTEP* **2020** (2020), no. 8 083C01.

[87] A. Denner, H. Eck, O. Hahn, and J. Kublbeck, *Compact Feynman rules for Majorana fermions*, *Phys. Lett. B* **291** (1992) 278–280.

Appendix A: Cross-Section Formulae

In this Appendix, we derive the full neutrino-neutrino scattering cross-section necessary for the calculations in the main text. The relevant Feynman diagrams stemming from the Lagrangian (1) are shown in Fig. 11: Figs. 11a to 11d correspond to neutrino-antineutrino scattering, and Figs. 11e and 11f to neutrino-neutrino scattering. p denote momenta and lowercase subindices denote mass eigenstates.
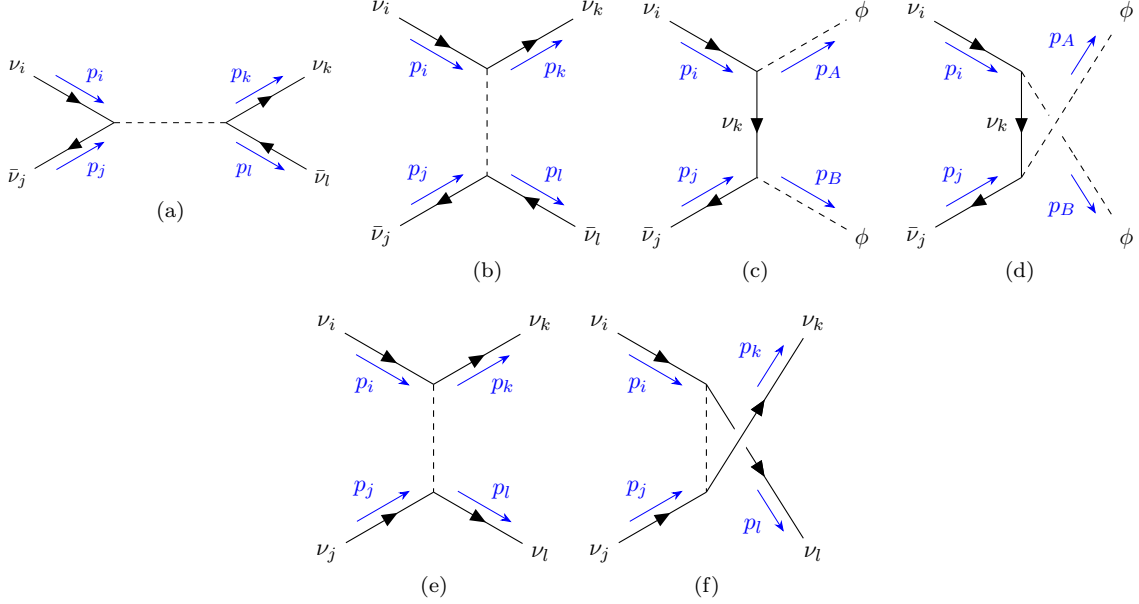

FIG. 11: Relevant Feynman diagrams for neutrino scattering at lowest order.

The amplitudes for the Feynman diagrams in Fig. 11 read

$$i\mathcal{M}_a = -ig^*_{ij}g_{kl}\,\frac{\bar{u}_k v_l \bar{v}_j u_i}{s - M^2_\phi + iM_\phi\Gamma_\phi}\,, \qquad (A1)$$

$$i\mathcal{M}_b = ig^*_{ik}g_{jl}\,\frac{\bar{u}_k u_i \bar{v}_l v_j}{t - M^2_\phi}\,, \qquad (A2)$$

$$i\mathcal{M}_c = -i\sum_k g^*_{ik}g_{jk}\,\bar{v}_j\frac{\slashed{p}_i - \slashed{p}_A + m_k}{t - m^2_k}u_i\,, \qquad (A3)$$

$$i\mathcal{M}_d = -i\sum_k g^*_{ik}g_{jk}\,\bar{v}_j\frac{\slashed{p}_i - \slashed{p}_B + m_k}{u - m^2_k}u_i\,, \qquad (A4)$$

$$i\mathcal{M}_e = ig^*_{ik}g^*_{jl}\,\frac{\bar{u}_k u_i \bar{u}_l u_j}{t - M^2_\phi}\,, \qquad (A5)$$

$$i\mathcal{M}_f = -ig^*_{il}g^*_{jk}\,\frac{\bar{u}_k u_j \bar{u}_l u_i}{u - M^2_\phi}\,, \qquad (A6)$$

where $g_{ij} = \sum_{\alpha,\beta} U^*_{\alpha i}U_{\beta j}g_{\alpha\beta}$ is the coupling strength in the mass basis, u and v are the standard Dirac spinors, s, t and u are the Mandelstam variables,[2] m_k is the mass of the k-th neutrino mass eigenstate, M_ϕ is the scalar mass, and Γ is the scalar decay width.

Our working assumptions are:

1. The incident neutrino is ultrarelativistic and left-handed (see Ref. [85] for the polarized scattering formalism).

2. We neglect CP violation (i.e., complex phases) in g_{ij}. One can check that, if the scalar couples to a single neutrino flavor, CP-violating effects are not present in neutrino-neutrino scattering.

3. The target neutrino is at rest and unpolarized.

---

[2] We define, for a neutrino final state, $t \equiv (p_i - p_k)^2$; and for a scalar final state, $t \equiv (p_i - p_A)^2$.

Under these assumptions, the differential scattering cross-section is given by [86]

$$\frac{\mathrm{d}\sigma}{\mathrm{d}t} = \left(\frac{1}{2}\right)\frac{1}{16\pi s^2}|\mathcal{M}|^2\,, \tag{A7}$$

where the $1/2$ factor applies for identical final-state particles. The kinematic limits for two neutrinos in the final state are $t \in [-s, 0]$, whereas for double scalar production $t \in \left[-\left(\sqrt{s}/2 + \sqrt{s/4 - M_\phi^2}\right), -\left(\sqrt{s}/2 - \sqrt{s/4 - M_\phi^2}\right)\right]$.

1. Dirac neutrinos

If neutrinos are Dirac fermions, and assuming that there is the same amount of target neutrinos and antineutrinos, the total inclusive cross-section for initial mass eigenstate i and final mass eigenstate j is given by

$$
\begin{aligned}
\sigma_{ij}(s) = \frac{1}{16\pi}\sum_{k,l}&\left[g_{ij}^2 g_{kl}^2\frac{s}{(s-M_\phi^2)^2 + M_\phi^2\Gamma^2} + \left(\frac{3}{2}\,g_{ik}^2 g_{jl}^2 + \frac{1}{2}\,g_{il}^2 g_{jk}^2\right)\left(\frac{s+2M_\phi^2}{s(s+M_\phi^2)} + 2\frac{M_\phi^2}{s^2}\log\frac{M_\phi^2}{M_\phi^2+s}\right)\right.\\
&\left.- g_{ij}g_{kl}g_{ik}g_{jl}\left(\frac{M_\phi^2}{s}-1\right)\frac{s+M_\phi^2\log\frac{M_\phi^2}{M_\phi^2+s}}{(s-M_\phi^2)^2+M_\phi^2\Gamma^2} + \frac{1}{2}\,g_{ik}g_{jl}g_{il}g_{jk}\left(\frac{1}{s}+\frac{2M_\phi^2(M_\phi^2+s)}{s^2(2M_\phi^2+s)}\log\frac{M_\phi^2}{M_\phi^2+s}\right)\right]\\
&+\frac{1}{64\pi s^2}\left(\sum_k g_{ik}^2 g_{jk}^2\right)\left\{\frac{s^2-4M_\phi^2 s+6M_\phi^4}{s-2M_\phi^2}\log\left[\left(\frac{\sqrt{s(s-4M_\phi^2)}+s-2M_\phi^2}{\sqrt{s(s-4M_\phi^2)}-s+2M_\phi^2}\right)^2\right] - 6\sqrt{s(s-4M_\phi^2)}\right\}.
\end{aligned}
\tag{A8}
$$

The first sum is the cross-section with two neutrinos in the final state, and the last term is the cross-section for double scalar production, present only if $s > 4M_\phi^2$.

For double neutrino production, we can classify the differential cross-section in terms of the visibility of the final state. Here, visible means that neutrinos must be left-handed and antineutrinos right-handed. We show the results in Table I.

	$\dfrac{\mathrm{d}\sigma}{\mathrm{d}t}$
k visible, l invisible	$\dfrac{1}{32\pi}\left[g_{ij}^2 g_{kl}^2\dfrac{1}{(s-M_\phi^2)^2+M_\phi^2\Gamma^2} + \left(\dfrac{1}{2}\right)g_{il}^2 g_{jk}^2\dfrac{u^2/s^2}{(u-M_\phi^2)^2}\right]$
k invisible, l invisible	$\dfrac{1}{32\pi}\left[\mathcal{S}_t\,g_{ik}^2 g_{jl}^2\dfrac{t^2/s^2}{(t-M_\phi^2)^2} + \left(\dfrac{1}{2}\right)\left(g_{il}^2 g_{jk}^2\dfrac{u^2/s^2}{(u-M_\phi^2)^2} + 2g_{ik}g_{jl}g_{il}g_{jk}\dfrac{t\cdot u/s^2}{(u-M_\phi^2)(t-M_\phi^2)}\right)\right]$
k invisible, l visible	$\dfrac{1}{32\pi}\left[g_{ij}^2 g_{kl}^2\dfrac{1}{(s-M_\phi^2)^2+M_\phi^2\Gamma^2} + \mathcal{S}_t\,g_{ik}^2 g_{jl}^2\dfrac{t^2/s^2}{(t-M_\phi^2)^2} + 2g_{ij}g_{kl}g_{ik}g_{jl}\dfrac{t(1-M_\phi^2/s)}{[(s-M_\phi^2)^2+M_\phi^2\Gamma^2](t-M_\phi^2)}\right]$
k visible, l visible	0

TABLE I: Total differential cross-section for double neutrino production, classified by the final state.

The $1/2$ factors are present if k=l, and

$$
\mathcal{S}_t \equiv \begin{cases} \frac{3}{2} & \text{if } k\neq l \\ 2 & \text{if } k = l \end{cases}. \tag{A9}
$$

For double scalar production, present only if $s > 4M_\phi^2$, the differential cross-section is given by

$$
\frac{\mathrm{d}\sigma}{\mathrm{d}t} = -\frac{1}{64\pi s^2}\left(\sum_k g_{ik}^2 g_{jk}^2\right)\frac{(-2M_\phi^2+s+2t)^2}{t^2(-2M_\phi^2+s+t)^2}\left[st + (t-M_\phi^2)^2\right]. \tag{A10}
$$

2. Majorana neutrinos

If neutrinos are Majorana fermions, there is no distinction between neutrinos and antineutrinos. Following Ref. [87], we obtain the total inclusive cross-section for initial mass eigenstate i and final mass eigenstate j as

$$\sigma_{ij}(s) = \frac{1}{16\pi} \sum_{k,l} \left[g_{ij}^2 g_{kl}^2 \frac{s}{(s - M_\phi^2)^2 + M_\phi^2 \Gamma^2} + \left(g_{ik}^2 g_{jl}^2 + g_{il}^2 g_{jk}^2 \right) \left(\frac{s + 2M_\phi^2}{s(s + M_\phi^2)} + 2 \frac{M_\phi^2}{s^2} \log \frac{M_\phi^2}{M_\phi^2 + s} \right) \right.$$
$$\left. - g_{ij}g_{kl}(g_{ik}g_{jl} + g_{il}g_{jk}) \left(\frac{M_\phi^2}{s} - 1 \right) \frac{s + M_\phi^2 \log \frac{M_\phi^2}{M_\phi^2+s}}{(s - M_\phi^2)^2 + M_\phi^2 \Gamma^2} + g_{ik}g_{jl}g_{il}g_{jk} \left(\frac{1}{s} + \frac{2M_\phi^2(M_\phi^2 + s)}{s^2(2M_\phi^2 + s)} \log \frac{M_\phi^2}{M_\phi^2 + s} \right) \right]$$
$$+ \frac{1}{32\pi s^2} \left(\sum_k g_{ik}^2 g_{jk}^2 \right) \left\{ \frac{s^2 - 4M_\phi^2 s + 6M_\phi^4}{s - 2M_\phi^2} \log \left[\left(\frac{\sqrt{s(s - 4M_\phi^2)} + s - 2M_\phi^2}{\sqrt{s(s - 4M_\phi^2)} - s + 2M_\phi^2} \right)^2 \right] - 6\sqrt{s(s - 4M_\phi^2)} \right\}, \tag{A11}$$

The first sum is the cross-section with two neutrinos in the final state, and the last term is the cross-section for double scalar production, present only if $s > 4M_\phi^2$.

The differential cross-section is simpler than in the Dirac neutrino case, as all final states are observable. For double neutrino production, we get

$$\frac{\mathrm{d}\sigma}{\mathrm{d}t} = \left(\frac{1}{2} \right) \frac{1}{8\pi} \left[g_{ij}^2 g_{kl}^2 \frac{1}{(s - M_\phi^2)^2 + M_\phi^2 \Gamma^2} + g_{ik}^2 g_{jl}^2 \frac{t^2/s^2}{(t - M_\phi^2)^2} + g_{il}^2 g_{jk}^2 \frac{u^2/s^2}{(u - M_\phi^2)^2} \right.$$
$$+ g_{ij}g_{kl}g_{ik}g_{jl} \frac{t(1 - M_\phi^2/s)}{[(s - M_\phi^2)^2 + M_\phi^2 \Gamma^2](t - M_\phi^2)} + g_{ik}g_{jl}g_{il}g_{jk} \frac{t \cdot u/s^2}{(u - M_\phi^2)(t - M_\phi^2)}$$
$$\left. + g_{ij}g_{kl}g_{il}g_{jk} \frac{u(1 - M_\phi^2/s)}{[(s - M_\phi^2)^2 + M_\phi^2 \Gamma^2](u - M_\phi^2)} \right], \tag{A12}$$

where the $1/2$ factor is present if $k = l$.

For double scalar production, present only if $s > 4M_\phi^2$, the differential cross-section is given by

$$\frac{\mathrm{d}\sigma}{\mathrm{d}t} = -\frac{1}{32\pi s^2} \left(\sum_k g_{ik}^2 g_{jk}^2 \right) \frac{(-2M_\phi^2 + s + 2t)^2}{t^2(-2M_\phi^2 + s + t)^2} \left[st + (t - M_\phi^2)^2 \right]. \tag{A13}$$

In all the expressions in this subsection, the cross-section must be multiplied by *half* the number of targets to obtain the number of events. In this convention the number of targets is the same for Dirac and Majorana neutrinos, assuming the same amount of target neutrinos and antineutrinos in the Dirac neutrino case.

3. Scalar decay

The only remaining calculation is the scalar decay width. At lowest order, it is mediated by the Feynman diagram in Fig. 12.
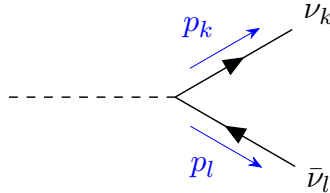

FIG. 12: Feynman diagram mediating scalar decay at lowest order.

The amplitude can be immediately computed

$$i\mathcal{M}_{\text{decay}} = -ig_{kl}\, \bar{u}_k v_l. \tag{A14}$$

Summing over final states, we get the total decay width [86]

$$\Gamma = \left(\frac{1}{2}\right) \frac{1}{8\pi} \frac{|\mathbf{p}_k|}{M_\phi^2} |\mathcal{M}|^2 = \left(\frac{1}{2}\right) \frac{M_\phi}{8\pi} \sum_{k,\,l} g_{kl}^2 \, , \tag{A15}$$

where the $1/2$ factor is present if neutrinos are Majorana fermions.

For the double scalar production process (Figs. 11c and 11d), we also need the differential decay width

$$\frac{1}{\Gamma} \frac{\mathrm{d}\Gamma}{\mathrm{d}E_k} = \frac{1}{\Gamma} \frac{\mathrm{d}\Gamma}{\mathrm{d}E_l} = \frac{1}{E_\phi} \, , \tag{A16}$$

where E_ϕ is the energy of the scalar. Unlike the total decay width, this computation is also valid if the scalar is not at rest. If neutrinos are Dirac fermions, one final state neutrino is visible and the other is invisible.